Supporting Information

Enhancing the magnetic relaxation through subcomponent self-assembly from linear Dy_2 to Dy_4 grid

Xiao-Lei Li,[ac‡] Zhifang Ma,[a‡] Jinjiang Wu,[ab] Quan Zhou,[ab] Jinkui Tang*[ab]

[a]State Key Laboratory of Rare Earth Resource Utilization, Changchun Institute of Applied Chemistry, Chinese Academy of Sciences, Changchun 130022, P. R. China

E-mail: tang@ciac.ac.cn

[b]School of Applied Chemistry and Engineering, University of Science and Technology of China, Hefei 230026, P. R. China

[c]Key Laboratory of Advanced Energy Materials Chemistry (Ministry of Education), College of Chemistry, Nankai University, Tianjin 300071, P. R. China

‡ These authors contributed equally to this work.

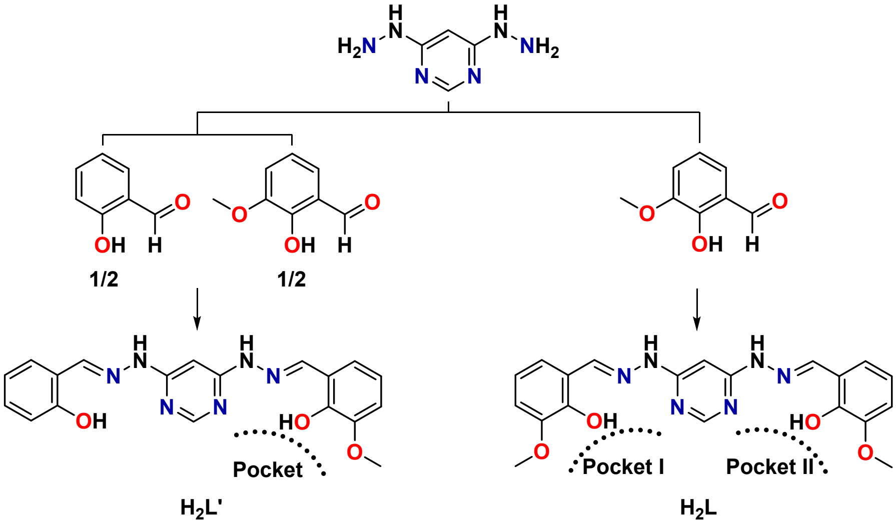

Scheme S1. Structures of the H_2L and H_2L' ligands and relative coordination pockets.

Table S1. Crystal data and structure refinement parameters for **1–4**.

Code	**1**	**2**	**3**	**4**
Formula	$C_{38}H_{60}Dy_2N_{16}O_{22}$	$C_{52}Dy_2H_{82}N_{12}O_{28}$	$C_{50}H_{62}Dy_2N_{12}O_{18.7}$	$C_{104}Dy_4H_{121}N_{14}Na_2O_{41}$
F_w(g mol^{-1})	1418.02	1648.29	1455.31	2919.12
Cryst syst	Monoclinic	Monoclinic	Monoclinic	Monoclinic
Space group	*C*2/c	*I*2/a	*P*2$_1$/c	*P*2$_1$
T (K)	296(2)	296(2)	296(2)	296(2)
a (Å)	21.314(5)	20.468(5)	11.3758(17)	12.3852(6)
b (Å)	14.009(3)	15.259(2)	12.797(2)	32.5128(16)
c (Å)	19.509(4)	24.156(3)	22.018(3)	15.4534(7)
α [°]	90	90	90	90
β [°]	105.499(4)	108.887(13)	100.741(3)	106.5540(10)
γ [°]	90	90	90	90
V(Å^3)	5613(2)	7138(2)	3149.1(8)	5964.8(5)
Cryst color	yellow	yellow	yellow	yellow
Z	4	4	2	2
μ(mm^{-1})	2.729	2.152	2.432	2.565
F(000)	2832	3056	1476	2738
R_{int}	0.0302	0.0395	0.0458	0.0524
*R_1 $[I > 2\sigma(I)]$	0.0277	0.0365	0.0378	0.056
*wR_2 $[I > 2\sigma(I)]$	0.0603	0.0962	0.0917	0.1165
*R_1 (all data)	0.0400	0.0447	0.0727	0.0805
*wR_2 (all data)	0.0667	0.1004	0.1095	0.1302
GOF	1.010	1.036	1.002	1.039

*$R_1 = \Sigma||Fo|-|Fc||/\Sigma|Fo|$ for $Fo > 2\sigma(Fo)$; $wR_2 = (\Sigma w(Fo^2-Fc^2)^2/\Sigma(wFc^2)^2)^{1/2}$ all reflections, $w = 1/[\sigma^2(Fo^2)+(0.1557P)^2]$ where $P = (Fo^2+2Fc^2)/3$

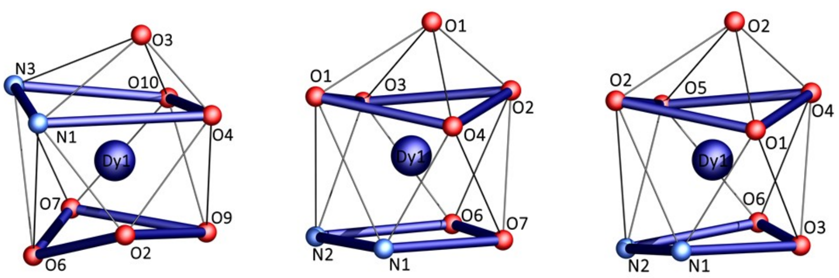

1 **2** **3**

Figure S1. Coordination polyhedra observed in **1–3**.

Table S2. Dy^{III} geometry analysis of **1–3** by SHAPE 2.1 software.[1]

Dy^{III}	MFF-9 (C_s)	CSAPR-9 (C_{4v})	TCTPR-9 (D_{3h})	JCSAPR-9 (C_{4v})	JTCTPR-9 (D_{3h})
Dy^{III}(1)	**2.345**	2.583	2.682	3.484	3.857
Dy^{III}(2)	1.938	**1.770**	2.797	1.956	3.362
Dy^{III}(3)	2.279	**2.232**	2.646	2.278	2.414

MFF-9 = Muffin; **CSAPR-9 = Spherical capped square antiprism**; TCTPR-9 = Spherical tricapped trigonal prism; JCSAPR-9 = Capped square antiprism J10; JTCTPR-9 = Tricapped trigonal prism J51.

Table S3: Selected bond Lengths and Dy···Dy distances in Å for **2** and **3**.

2			**3**		
Atoms	Atoms	Length	Atoms	Atoms	Length
Dy1	O1	2.224(7)	Dy1	O1	2.228(4)
Dy1	O2	2.319(9)	Dy1	O2	2.321(5)
Dy1	$O2^1$	2.643(8)	Dy1	$O2^2$	2.706(5)
Dy1	$O3^1$	2.436(9)	Dy1	$O3^2$	2.409(5)
Dy1	O4	2.402(8)	Dy1	O4	2.391(4)
Dy1	O5	2.431(9)	Dy1	O5	2.371(5)
Dy1	O6	2.441(9)	Dy1	O6	2.556(5)
Dy1	N1	2.554(10)	Dy1	N1	2.573(6)
Dy1	N2	2.524(9)	Dy1	N2	2.481(3)
Dy1	**$Dy1^1$**	**4.126(3)**	**Dy1**	**$Dy1^2$**	**4.171(2)**

^{1}1/2-x,3/2-y,3/2-z, ^{2}1-x,1-y,1-z

Table S4. Selected bond Angles in ° for **2** and **3**.

2				**3**			
Atoms	Atoms	Atoms	Angle/°	Atoms	Atoms	Atoms	Angle/°
O1	Dy1	O2	83.1(3)	O1	Dy1	O2	83.18(16)
O1	Dy1	$O2^1$	70.4(3)	O1	Dy1	$O2^2$	69.80(14)
O1	Dy1	$O3^1$	80.9(3)	O1	Dy1	$O3^2$	79.82(17)
O1	Dy1	O4	139.0(3)	O1	Dy1	O4	138.47(17)
O1	Dy1	O5	84.4(3)	O1	Dy1	O5	87.10(17)
O1	Dy1	O6	135.6(3)	O1	Dy1	O6	135.69(17)
O1	Dy1	N1	70.1(3)	O1	Dy1	N1	69.55(17)
O1	Dy1	N2	130.9(3)	O1	Dy1	N2	131.93(15)
O2	Dy1	$O2^1$	67.7(3)	O2	Dy1	$O2^2$	68.12(18)
O2	Dy1	$O3^1$	118.6(3)	O2	Dy1	$O3^2$	117.82(18)
O2	Dy1	O4	74.0(3)	O2	Dy1	O4	73.34(14)
O2	Dy1	O5	158.3(3)	O2	Dy1	O5	158.96(17)
O2	Dy1	O6	141.3(3)	O2	Dy1	O6	141.01(15)
O2	Dy1	N1	88.3(3)	O2	Dy1	N1	85.55(18)
O2	Dy1	N2	78.2(3)	O2	Dy1	N2	83.47(15)
$O3^1$	Dy1	$O2^1$	51.1(3)	$O3^1$	Dy1	$O2^2$	49.83(17)

O3^{1}	Dy1	O6	78.2(3)	O3^{1}	Dy1	O6	75.36(18)
O3^{1}	Dy1	N1	137.8(3)	O3^{1}	Dy1	N1	138.99(18)
O3^{1}	Dy1	N2	147.4(3)	O3^{1}	Dy1	N2	145.71(15)
O4	Dy1	O2^{1}	69.6(2)	O4	Dy1	O2^{2}	69.80(13)
O4	Dy1	O3^{1}	81.0(3)	O4	Dy1	O3^{2}	81.59(16)
O4	Dy1	O6	75.0(3)	O4	Dy1	O6	72.81(15)
O4	Dy1	O5	126.1(3)	O4	Dy1	O5	124.75(16)
O4	Dy1	N1	140.4(3)	O4	Dy1	N1	139.25(17)
O4	Dy1	N2	77.2(3)	O4	Dy1	N2	79.47(14)
O5	Dy1	O2^{1}	123.9(3)	O5	Dy1	O2^{2}	125.39(17)
O5	Dy1	O3^{1}	76.6(3)	O5	Dy1	O3^{2}	78.42(19)
O5	Dy1	O6	52.8(3)	O5	Dy1	O6	52.44(17)
O5	Dy1	N1	70.8(3)	O5	Dy1	N1	73.56(19)
O5	Dy1	N2	97.1(3)	O5	Dy1	N2	89.31(17)
O6	Dy1	O2^{1}	120.8(3)	O6	Dy1	O2^{2}	116.23(16)
O6	Dy1	N1	101.5(3)	O6	Dy1	N1	108.40(18)
O6	Dy1	N2	72.9(3)	O6	Dy1	N2	71.85(16)
N1	Dy1	O2^{1}	135.6(3)	N1	Dy1	O2^{2}	133.51(15)
N2	Dy1	O2^{1}	137.4(3)	N2	Dy1	O2^{2}	142.71(14)
N2	Dy1	N1	64.4(3)	N2	Dy1	N1	63.51(15)
N3	N1	Dy1	116.9(7)	N3	N1	Dy1	117.3(4)
Dy1	**O2**	**Dy1^{1}**	**112.3(3)**	**Dy1**	**O2**	**Dy1^{2}**	**111.88(18)**

^{1}1/2-x,3/2-y,3/2-z, ^{2}1-x,1-y,1-z

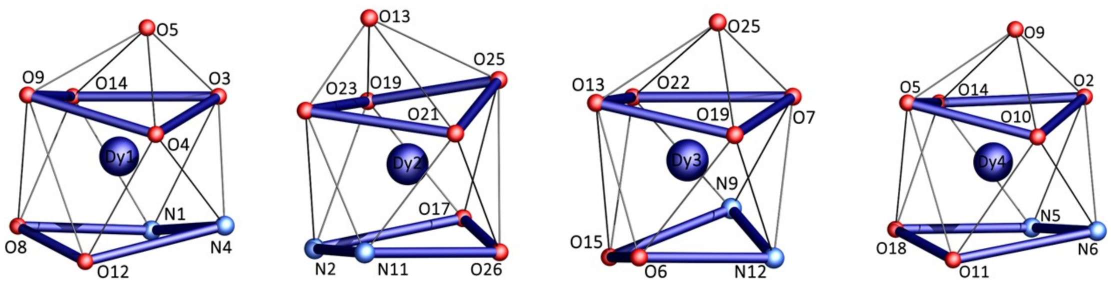

Figure S2. Coordination polyhedra observed in **4**.

Table S5. Dy^{III} geometry analysis of **4** by SHAPE 2.1 software.[1]

Dy^{III}	**MFF-9 (C_s)**	**CSAPR-9 (C_{4v})**	**TCTPR-9 (D_{3h})**	**JCSAPR-9 (C_{4v})**	**JTCTPR-9 (D_{3h})**
Dy^{III}(1)	**1.954**	2.525	3.290	3.052	2.687
Dy^{III}(2)	2.938	2.912	3.470	**2.386**	2.886
Dy^{III}(3)	**1.980**	2.315	3.000	2.873	2.408
Dy^{III}(4)	2.293	2.237	2.806	**2.165**	2.824

MFF-9 = Muffin; CSAPR-9 = Spherical capped square antiprism; TCTPR-9 = Spherical tricapped trigonal prism; **JCSAPR-9 = Capped square antiprism J10**; JTCTPR-9 = Tricapped trigonal prism J51.

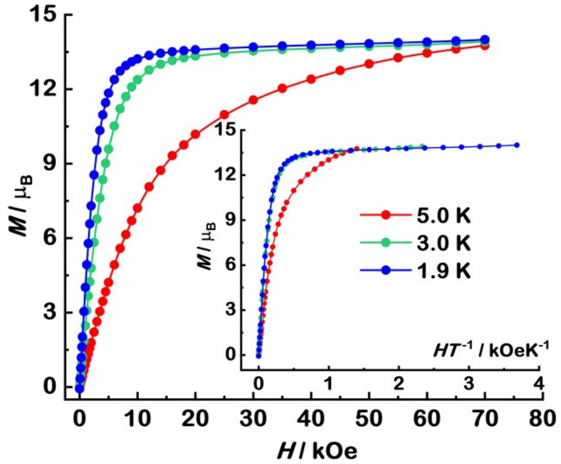

Figure S3. Field dependences of magnetization in the field range 0−70 kOe and temperature range 1.9−5.0 K for **1**. Inset: Plots of the reduced magnetization *M* versus *H*/*T*.

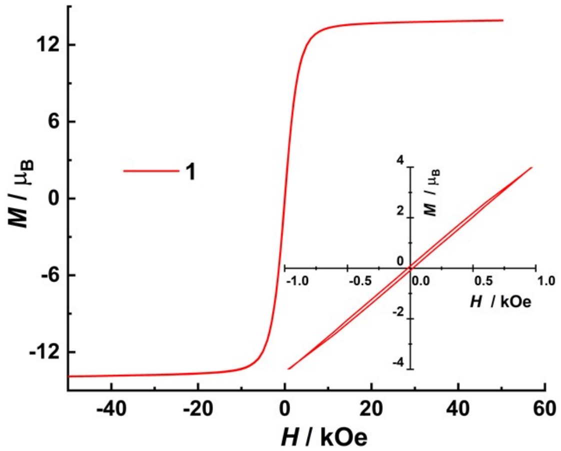

Figure S4. *M* (*H*) hysteresis for **1** using a scan rate of 2.0 mTs^{-1}.

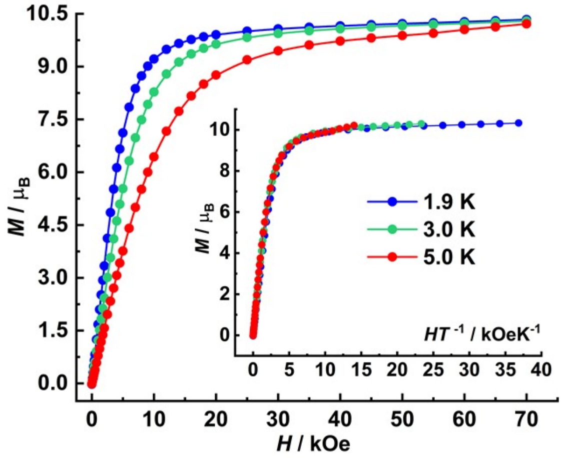

Figure S5. Field dependences of magnetization in the field range 0−70 kOe and temperature range 1.9−5.0 K for **2**. Inset: Plots of the reduced magnetization *M* versus *H*/*T*.

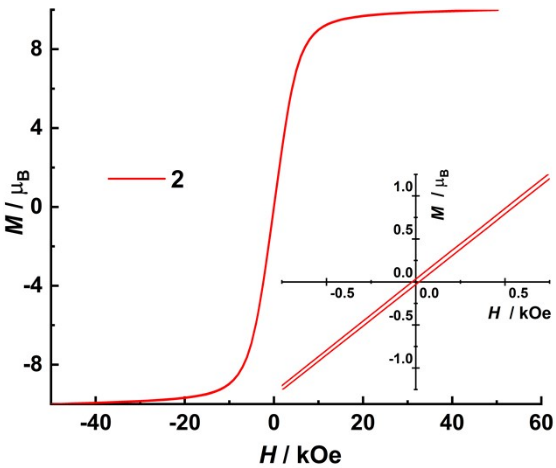

Figure S6. *M* (*H*) hysteresis for **2** using a scan rate of 2.0 mTs^{-1}.

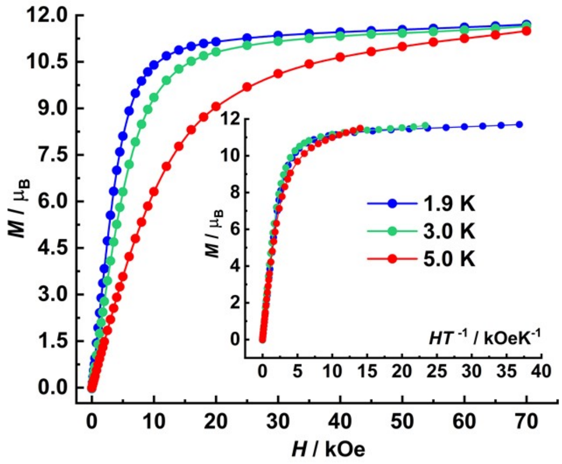

Figure S7. Field dependences of magnetization in the field range 0−70 kOe and temperature range 1.9−5.0 K for **3**. Inset: Plots of the reduced magnetization *M* versus *H*/*T*.

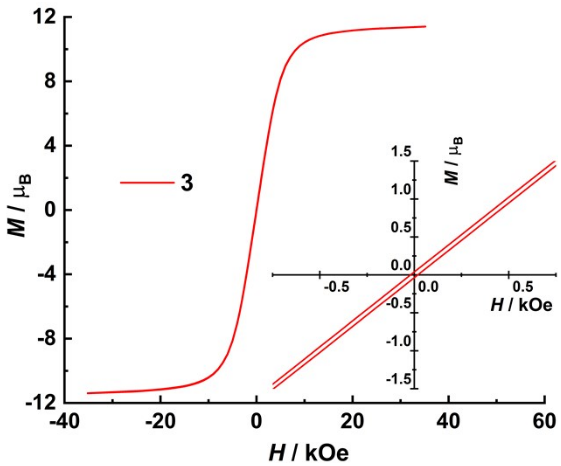

Figure S8. *M* (*H*) hysteresis for **3** using a scan rate of 2.0 mTs^{-1}.

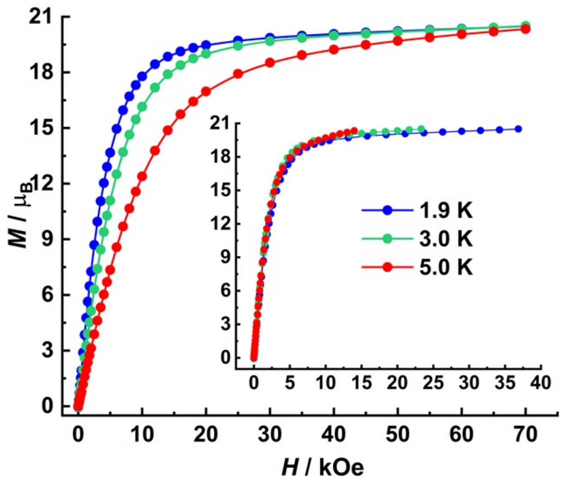

Figure S9. Field dependences of magnetization in the field range 0−70 kOe and temperature range 1.9−5.0 K for **4**. Inset: Plots of the reduced magnetization *M* versus *H*/*T*.

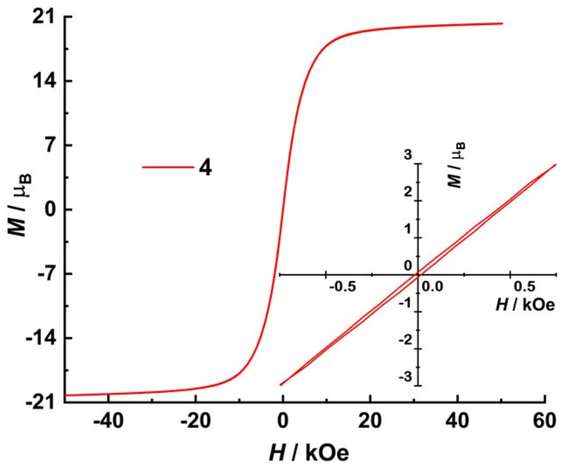

Figure S10. *M* (*H*) hysteresis for **4** using a scan rate of 2.0 mTs^{-1}.

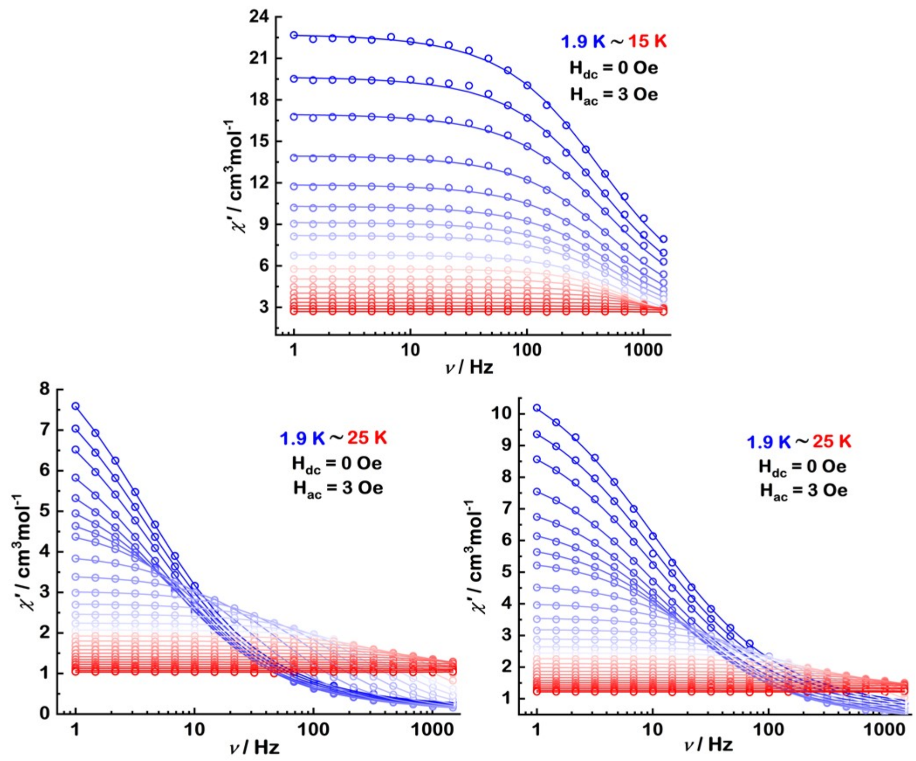

Figure S11. Frequency dependence of the in-phase (χ') ac susceptibility signals for **1–3** (from top, bottom left to right) under zero-dc field. The solid lines correspond to the best fit.

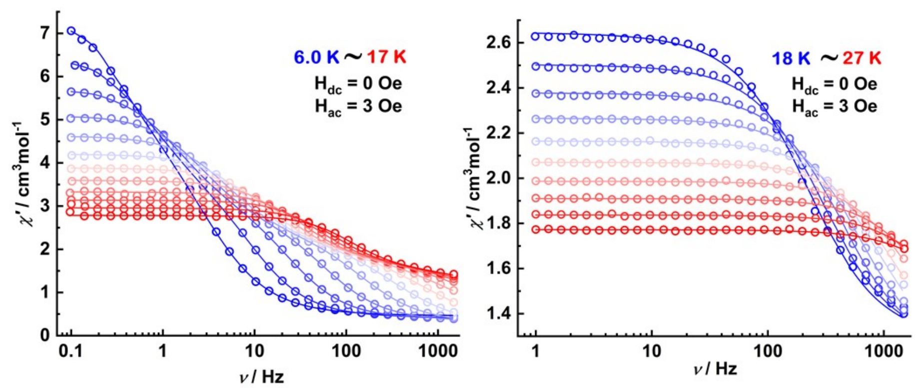

Figure S12. Frequency dependence of the in-phase (χ') ac susceptibility signals for **4** under zero-dc field. The solid lines correspond to the best fit.

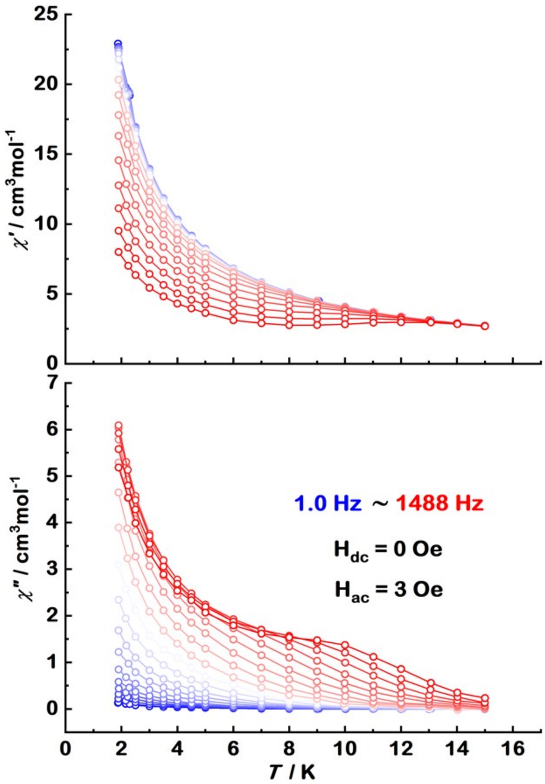

Figure S13. Plots of ac susceptibility vs. temperature at H_{ac} = 3.5 Oe, H_{dc} = 0 Oe, oscillating at 1−1488 Hz for **1** in the temperature range of 1.9−15 K.

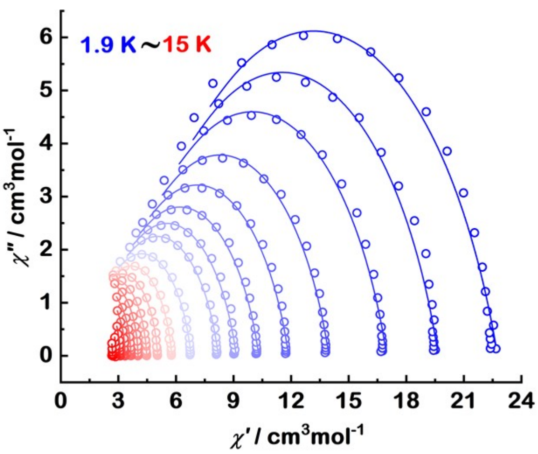

Figure S14. Cole−Cole plots for temperatures between 1.9 and 15 K under a zero dc field with the best fit to the generalized Debye model for **1**. The Solid lines represent fits to the data, as described in the main text.

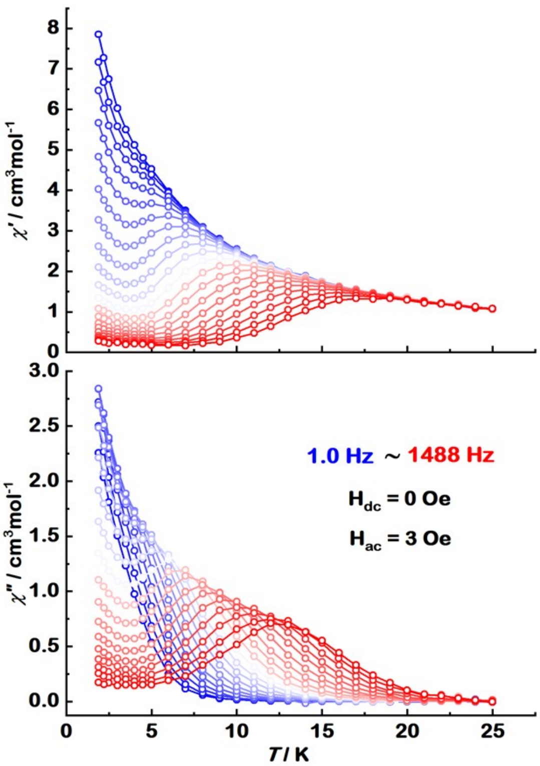

Figure S15. Plots of ac susceptibility vs. temperature at H_{ac} = 3.5 Oe, H_{dc} = 0 Oe, oscillating at 1−1488 Hz for **2** in the temperature range of 1.9−15 K.

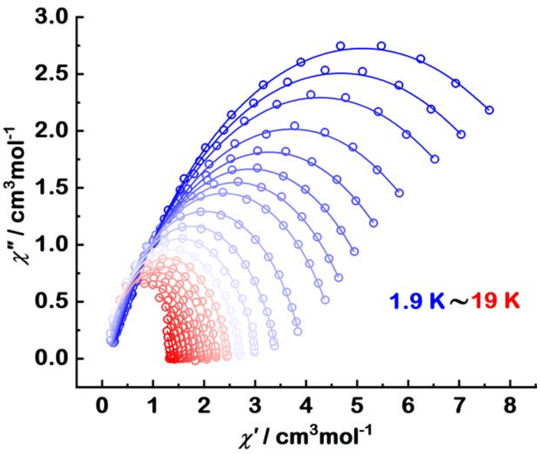

Figure S16. Cole−Cole plots for temperatures between 1.9 and 15 K under a zero dc field with the best fit to the generalized Debye model for **2**. The Solid lines represent fits to the data, as described in the main text.

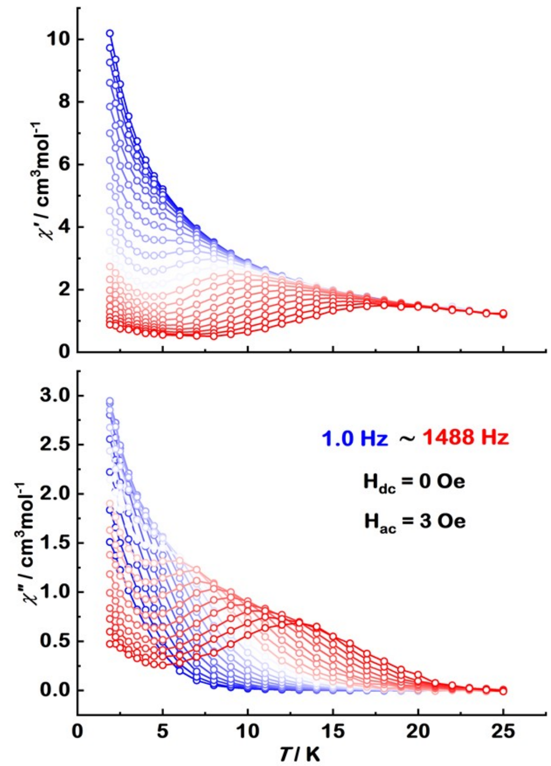

Figure S17. Plots of ac susceptibility vs. temperature at H_{ac} = 3.5 Oe, H_{dc} = 0 Oe, oscillating at 1−1488 Hz for **3** in the temperature range of 1.9−25 K.

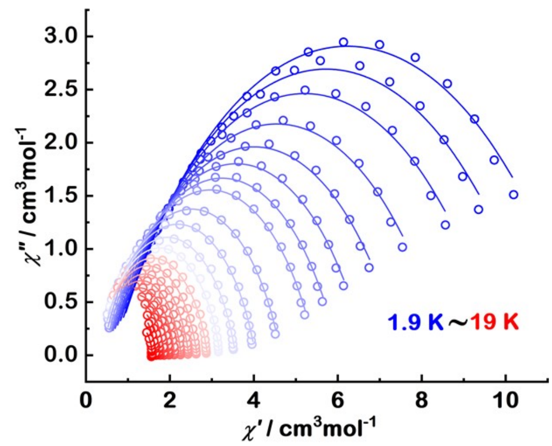

Figure S18. Cole−Cole plots for temperatures between 1.9 and 19 K under a zero dc field with the best fit to the generalized Debye model for **3**. The Solid lines represent fits to the data, as described in the main text.

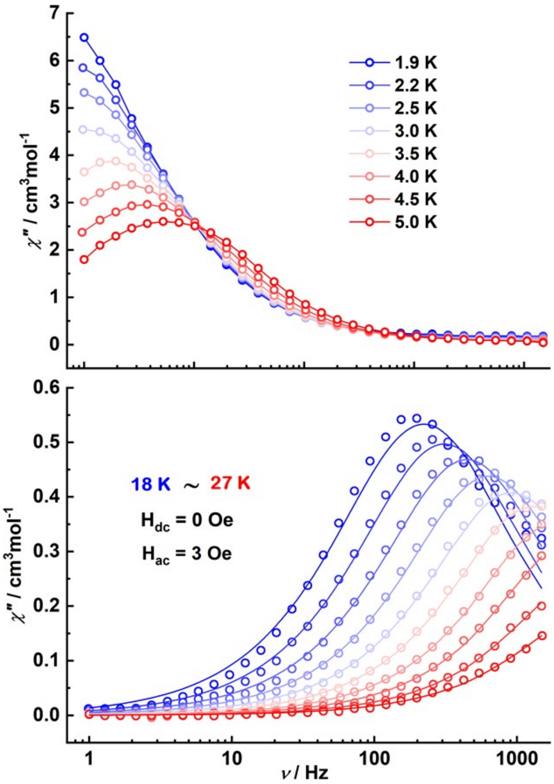

Figure S19. Frequency dependence of the out-of-phase (*χ″*) ac susceptibility signals for complex **4** between 1.9−5.0 K (top) and 18−27 K (bottom) under zero-dc field. The solid lines are guide for eyes (top) and correspond to the best fit (bottom).

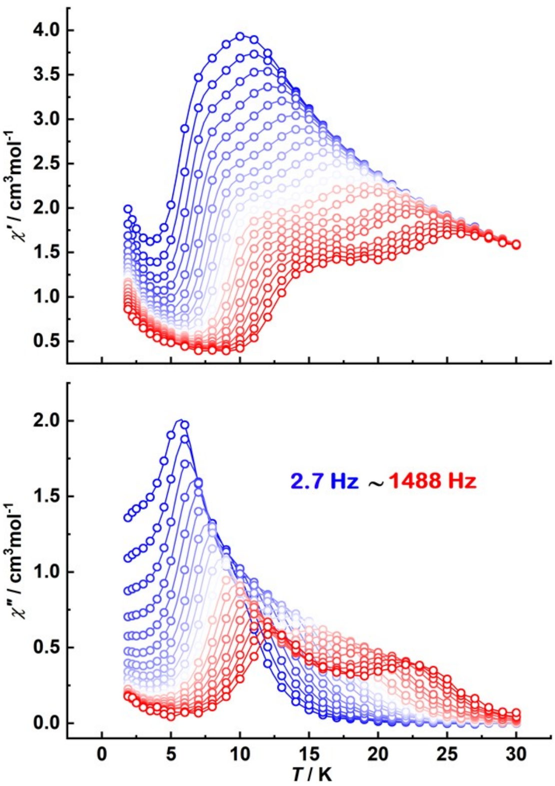

Figure S21. Plots of ac susceptibility vs. temperature at H_{ac} = 3.5 Oe, H_{dc} = 0 Oe, oscillating at 1−1488 Hz for **4** in the temperature range of 1.9−30 K.

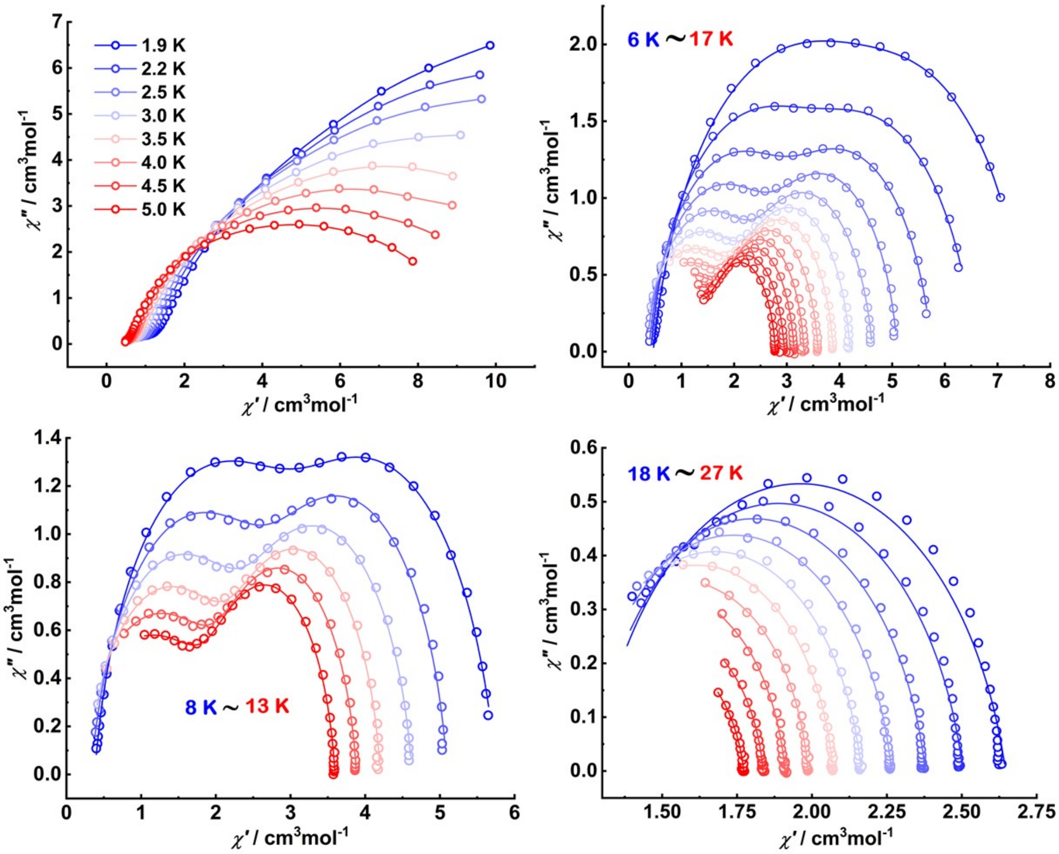

Figure S20. Cole−Cole plots for temperatures between 1.9 and 27 K under a zero dc field with the best fit to the generalized Debye model for **4**. The Solid lines represent fits to the data, as described in the main text.

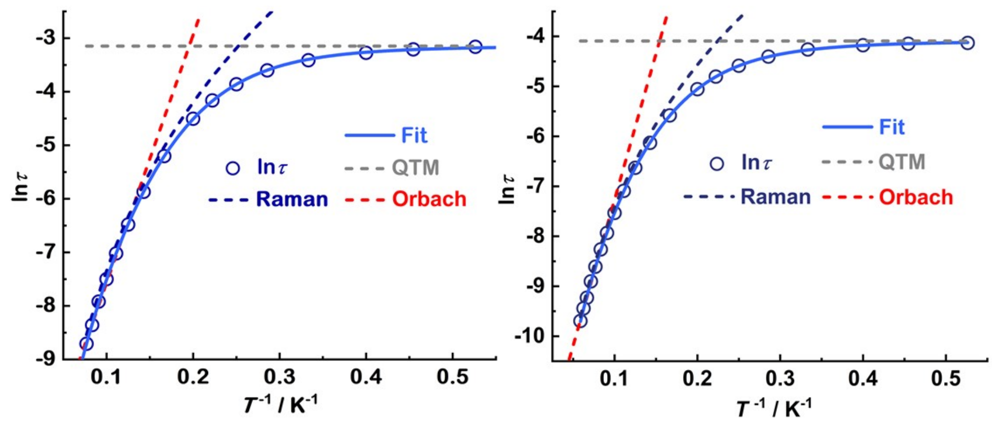

Figure S22. The plots of lnτ versus T^{-1} for **2** (left) and **3** (right) under zero DC field. The blue lines represent the fit to multiple relaxation processes using Equation 1 (main text).

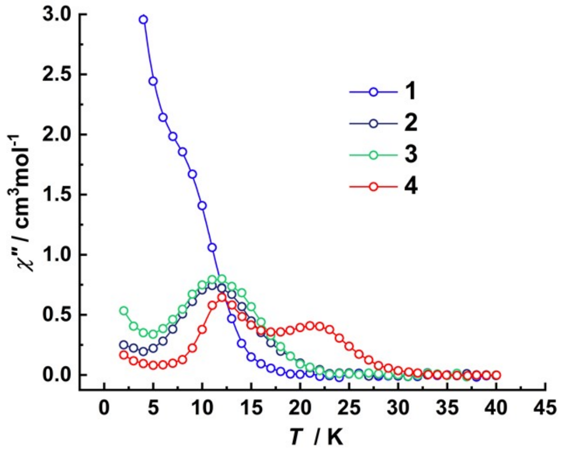

Figure S23. Temperature dependence of the (χ'') ac susceptibility components under zero dc-field and at 1000 Hz ac frequency for **1−4**.

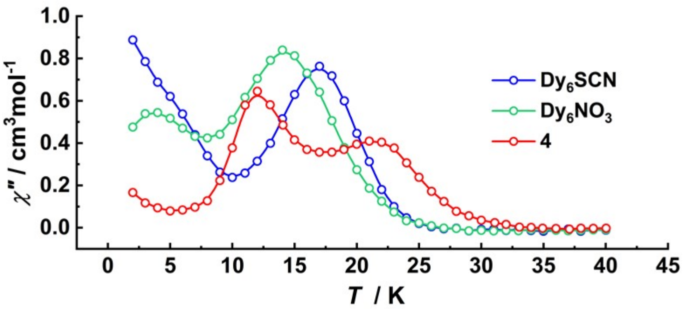

Figure S24. Temperature dependence of the (χ'') ac susceptibility components under zero dc-field and at 1000 Hz ac frequency for **Dy_6–SCN**, **Dy_6–NO_3** and **4**, respectively.

Table S6. Fitting parameters for complexes **1−4**.

Complex	U_{eff} (K)	τ_0 (s)	n	C ($s^{-1}K^{-n}$)	τ_{QTM}
1	52.45	8.2E−7	0.39	2053.7	–
2	56.04	1.5E−5	4.54	0.04	23.26
3	58.4	2.3E−5	4.12	0.13	59.9
4−S	207.25	2.17E−8	5.36	1.38E-4	–
4−F	94.98	7.48E-8	2.33	0.32	–

Table S6. The best fitting parameters for Cole−Cole plots of **1** at varying temperatures under zero applied dc field.

T (K)	χ_T	χ_S	α
1.9	0.227586E+02	0.357018E+01	0.271767E+00
2.2	0.196683E+02	0.340381E+01	0.254382E+00
2.5	0.169818E+02	0.298057E+01	0.254387E+00
3.0	0.139689E+02	0.262926E+01	0.244757E+00
3.5	0.118677E+02	0.233606E+01	0.237717E+00
4.0	0.103180E+02	0.210783E+01	0.231018E+00
4.5	0.914134E+01	0.192328E+01	0.223195E+00

5.0	0.820376E+01	0.186075E+01	0.207630E+00
6.0	0.678492E+01	0.164347E+01	0.174419E+00
7.0	0.578554E+01	0.151139E+01	0.138300E+00
8.0	0.504774E+01	0.136657E+01	0.102457E+00
9.0	0.447631E+01	0.114663E+01	0.826008E-01
10.0	0.402747E+01	0.103917E+01	0.527822E-01
11.0	0.365401E+01	0.105726E+01	0.320280E-01
12.0	0.335382E+01	0.102295E+01	0.204712E-01

Table S7. The best fitting parameters for Cole−Cole plots of **2** at varying temperatures under zero applied dc field.

T (K)	χ_T	χ_S	α
1.9	0.171003E+00	0.100318E+02	0.164636E+01
2.2	0.159463E+00	0.919902E+01	0.164831E+01
2.5	0.145334E+00	0.838580E+01	0.165014E+01
3.0	0.142188E+00	0.729271E+01	0.165735E+01
3.5	0.134370E+00	0.641740E+01	0.167059E+01
4.0	0.131785E+00	0.569463E+01	0.169133E+01
4.5	0.124097E+00	0.513443E+01	0.170899E+01
5.0	0.107110E+00	0.467705E+01	0.172566E+01
6.0	0.771950E-01	0.396440E+01	0.175317E+01
7.0	0.601547E-01	0.343909E+01	0.177381E+01
8.0	0.474027E-01	0.303628E+01	0.178783E+01
9.0	0.355674E-01	0.272397E+01	0.179585E+01
10.0	0.566129E-01	0.246678E+01	0.181081E+01
11.0	0.109211E+00	0.224408E+01	0.183258E+01
12.0	0.795037E-01	0.207612E+01	0.183300E+01
13.0	0.168688E+00	0.192526E+01	0.185098E+01
14.0	0.161811E+00	0.180060E+01	0.184752E+01
15.0	0.330864E+00	0.168483E+01	0.187441E+01

Table S8. The best fitting parameters for Cole−Cole plots of **3** at varying temperatures under zero applied dc field.

T (K)	χ_T	χ_S	α
1.9	0.118181E+02	0.651389E+00	0.385484E+00
2.2	0.108141E+02	0.635213E+00	0.377203E+00
2.5	0.983229E+01	0.592191E+00	0.373231E+00
3.0	0.853979E+01	0.559666E+00	0.360667E+00
3.5	0.748813E+01	0.533324E+00	0.342416E+00
4.0	0.665870E+01	0.506701E+00	0.320999E+00
4.5	0.601167E+01	0.474169E+00	0.305736E+00
5.0	0.547827E+01	0.433742E+00	0.291645E+00
6.0	0.464239E+01	0.388551E+00	0.263726E+00
7.0	0.403487E+01	0.338893E+00	0.245252E+00

8.0	0.356558E+01	0.316252E+00	0.230952E+00
9.0	0.319560E+01	0.314798E+00	0.215004E+00
10.0	0.289643E+01	0.296170E+00	0.212955E+00
11.0	0.264526E+01	0.303098E+00	0.199851E+00
12.0	0.244721E+01	0.353062E+00	0.190454E+00
13.0	0.226761E+01	0.380754E+00	0.178071E+00
14.0	0.211095E+01	0.457728E+00	0.159387E+00
15.0	0.198436E+01	0.521282E+00	0.163042E+00
16.0	0.186440E+01	0.651555E+00	0.132895E+00
17.0	0.175776E+01	0.762406E+00	0.109855E+00

Table S9. The best fitting parameters for Cole−Cole plots of **4** at varying temperatures under zero applied dc field.

T (K)	$\chi_{S, tot}$	$\Delta\chi_1$	$\Delta\chi_2$	α_1	α_2
6	0.462837	4.19811	2.88344	0.185820	0.118835
7	0.416741	2.99136	3.14972	0.144294	0.176163
8	0.379799	2.61702	2.75098	0.141080	0.150949
9	0.330834	2.39851	2.36889	0.160744	0.116412
10	0.289189	2.09119	2.24583	0.172721	0.129173
11	0.233489	1.99534	1.97349	0.219124	0.106147
12	0.0992182	2.05558	1.72896	0.309237	0.0909898
13	0.0314589	2.03966	1.52711	0.374204	0.0750385
14	0.0979910	1.85857	1.37323	0.388724	0.0515124
15	0.466148	1.36701	1.30570	0.348105	0.0588868
16	0.507442	1.28684	1.16478	0.407458	0.0515513
17	0.359484	1.28684	1.13806	0.370810	0.0589097

Table S9. The best fitting parameters for Cole−Cole plots of **4** at varying temperatures under zero applied dc field.

T (K)	χ_T	χ_S	α
18	0.264590E+01	0.127840E+01	0.152779E+00
19	0.250340E+01	0.127067E+01	0.132313E+00
20	0.237798E+01	0.123387E+01	0.122385E+00
21	0.226533E+01	0.121197E+01	0.112417E+00
22	0.216458E+01	0.118878E+01	0.109850E+00
23	0.207047E+01	0.117433E+01	0.971040E-01
24	0.198631E+01	0.117843E+01	0.882146E-01
25	0.190982E+01	0.114476E+01	0.977433E-01
26	0.183695E+01	0.123402E+01	0.985308E-01
27	0.177229E+01	0.126416E+01	0.126150E+00

References

1. D. Casanova, M. Llunell, P. Alemany and S. Alvarez, *Chem. Eur. J.*, 2005, **11,** 1479-1494.